

Seabird range contraction and dispersal under climate change

Received: 28 May 2025

Accepted: 22 April 2026

Published online: 19 May 2026

 Check for updates


Jorge Avaria-Llautureo ^{1,2} , Marcelo M. Rivadeneira ^{3,4}, Chris Venditti¹ & Guillermo Luna-Jorquera ^{2,4,5} 

Many marine ectotherms have responded to local warming through body-size reductions and dispersal to optimal environments. However, whether endothermic marine species, such as seabirds, exhibit similar responses remains unclear owing to gaps in literature that hinder comprehensive global assessments. Here we show that globally distributed seabirds (albatrosses, petrels, shearwaters and storm petrels) facing rapid historical climate change responded with changes in geographic range size rather than body mass. In addition, under higher rates of climate change, species' ranges contracted most, forcing these species to disperse longer distances. These historical inferences align with expected responses to modern climate change, as over 70% of extant species contract their ranges and disperse farther under a climate scenario leading to severe warming by 2100. These results underscore the urgent need to integrate range dynamics into conservation strategies and reveal that the rate of climate change poses the greatest threat to seabird diversity.

Seabirds are critical to marine ecosystems and human economies by virtue of their roles in nutrient cycling and fisheries support¹ but they are highly threatened by climate change^{2–4}. Climate change impacts seabirds both indirectly, through shifts in prey distribution and abundance, and directly, via changes in demographic, life-history and ecological traits^{2,5,6}. For example, many seabirds from the Northern Hemisphere are struggling to breed successfully owing to ocean warming and human impacts⁷. However, key gaps persist in the understanding of seabirds' global responses to climate change, particularly for tropical and subtropical Procellariiformes^{2,5,6} (pelagic seabirds that include albatrosses, petrels, shearwaters and storm petrels). This gap is hard to fill by extrapolations from high-latitude observations because seabird responses to climate change vary across regions⁶. In addition, field studies often require more than two decades of observations to detect global trends⁶, further complicating global inferences⁶.

Phylogenetic comparative methods offer a unique approach to fill these gaps by allowing the inference of long-term, historical responses to climate change from global species-level data. Such comparative approaches provide a framework to test whether species

are more likely to respond through changes in body size⁸, range shifts⁹ and/or geographic range size¹⁰, often known as the universal responses of species to modern climate change. Regarding body size, higher local temperature (LT) is expected to drive species size reductions in both ectotherms and endotherms by means of different thermoregulatory mechanisms^{11–13}. Ectothermic body temperature and metabolic rate scales directly with LT^{14,15}; for example, a tropical fish at 30 °C requires six times more oxygen for resting metabolism than a polar fish at 0 °C (ref. 14). Warmer conditions thus increase energetic demands, favouring smaller species with reduced total energy expenditure¹⁶. Conversely, endotherms such as seabirds maintain stable metabolic rates across a wide LT range (the thermoneutral zone) with increases only outside this range^{11,12,15}. Under warmer conditions, a smaller body size facilitates heat dissipation, which may select for smaller seabirds over evolutionary time¹⁷. However, our analysis shows that LT explains only ~6% of body mass variation in extant Procellariiformes (Extended Data Fig. 1), suggesting that body-size reduction might not be a survival strategy against rising temperatures.

¹School of Biological Sciences, University of Reading, Reading, UK. ²Center for Ecology and Sustainable Management of Oceanic Islands, Coquimbo, Chile. ³Departamento de Biología, Facultad de Ciencias, Universidad de La Serena, La Serena, Chile. ⁴Centro de Estudios Avanzados en Zonas Áridas, Coquimbo, Chile. ⁵Departamento de Biología Marina, Universidad Católica del Norte, Coquimbo, Chile.  e-mail: j.l.avaria@reading.ac.uk; gluna@ucn.cl

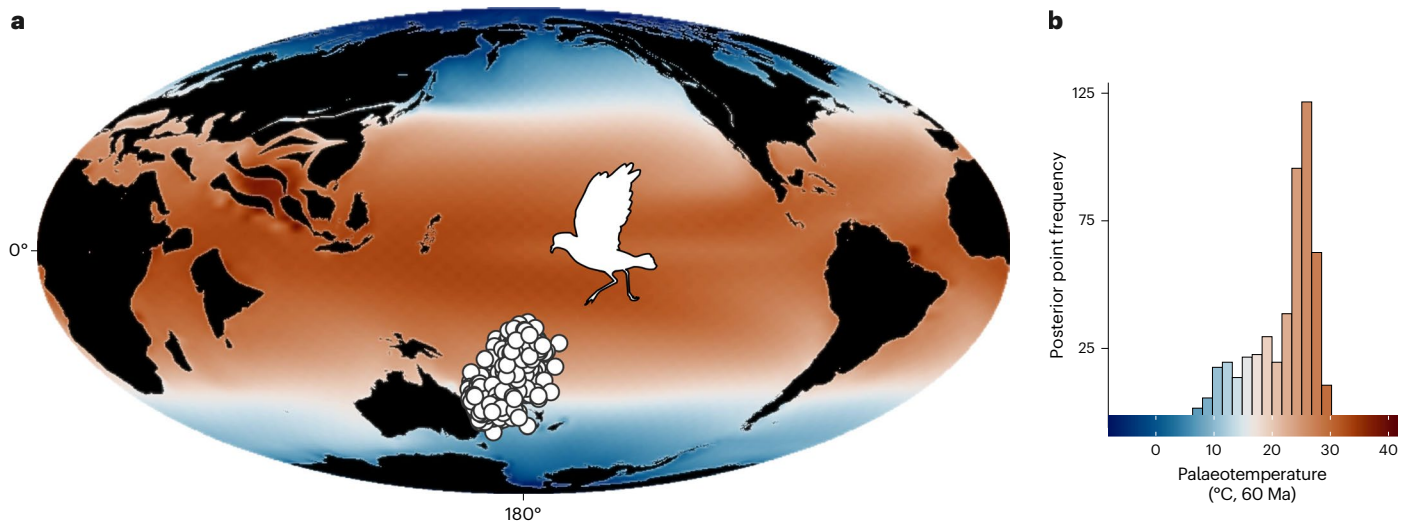


Fig. 1 | Procellariiformes' MRCA location and temperature. a, Global palaeomap showing reconstructed 2-m palaeotemperatures with the posterior distribution of the MRCA geographic coordinates (white points) inferred with the Geo model. The MRCA was located in what is now the Coral Sea, east of Australia.

b, Distribution of 2-m palaeotemperatures extracted at the MRCA posterior coordinates, indicating occupation of temperate to warm environments ($n = 500$ coordinates; 500 temperature data points). Data from ref. 45. Credit: *Oceanites* icon, Carlos Jeri, PhyloPic under a Creative Commons license CC0 1.0.

An alternative response to contemporary climate change is species range shifts, whereby species alter their geographic distributions through contractions at trailing range edges and expansions at leading range edges^{10,16,18,19}. For seabirds, range shifts are expected to predominate over local adaptation. This is because seabirds have limited capacity for local adaptation: they typically operate near their maximum physiological tolerance for ambient temperature within a narrow thermal range^{11,12}. As a result, they are highly susceptible to local climate change, such that even minor temperature increases can exceed their coping capacity^{11,12}. In such cases, dispersal to new areas represents a viable survival strategy. In addition, the high vagility of seabirds, which enables them to disperse across entire oceans^{20,21}, further supports the expectation that range shift will predominate over local adaptation in the face of climate change. Unfortunately, the scarcity of data on seabird range shifts has so far prevented rigorous tests of this prediction². For example, the BioShifts database²² includes records for only 15 species of Procellariiformes, representing just ~10% of the group's total diversity. To address this gap, we reconstruct the long-term historical dispersal routes of Procellariiformes using the phylogenetic Geographical (Geo) model in BayesTraits^{23–25} (Methods). We refer to these historical routes as 'species dispersal' to distinguish them from contemporary responses.

Increased species dispersal distance can directly impact gene flow among populations and, consequently, speciation rate through genetic divergence²⁶. However, predicting the outcome is complex. Highly dispersive individuals may either maintain gene flow among populations, thereby decreasing speciation rates, or colonize distant areas, potentially increasing speciation rates through subsequent isolation²⁶. In environmentally homogeneous regions, dispersal may sustain population connectivity and thereby inhibit speciation. By contrast, in heterogeneous regions, long-distance dispersal may enable individuals to cross geographic barriers, increasing the probability of allopatric speciation by separating populations through physical barriers (that is, vicariance). While broad-scale studies across the avian clade indicate that longer dispersal distances generally inhibit^{26,27} or have minimal impact²⁸ on speciation rates, research focused on shearwaters has shown the opposite pattern²⁹, with long-distance dispersal promoting diversification. Given this seabird-specific evidence, we expect a positive relationship between dispersal distance and speciation rate in Procellariiformes.

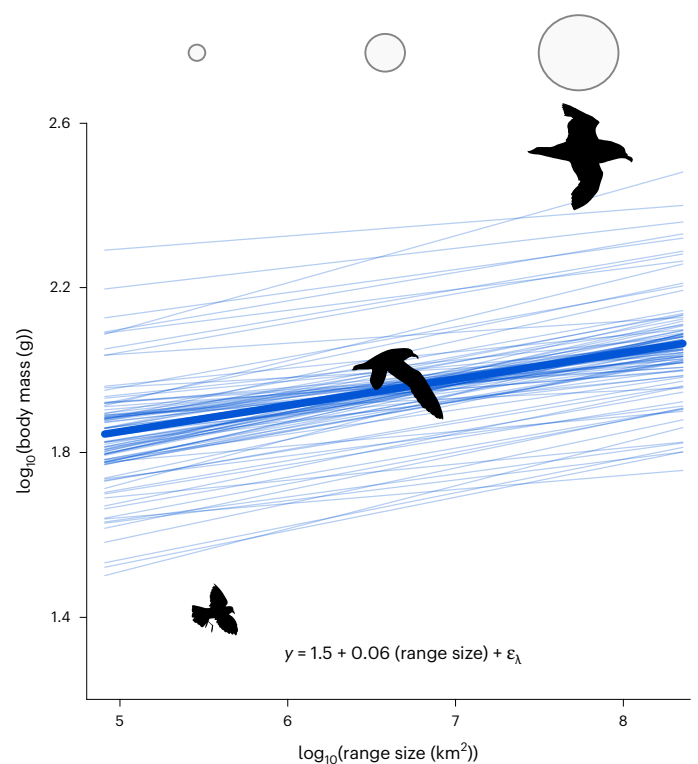


Fig. 2 | Larger seabirds are geographically more widespread. The plot shows the predicted body mass by range size (pMCMC_{99.6} >95). Light transparent lines indicate the posterior regression lines linking body mass with range size. The dark line indicates the mean regression line obtained from the inset model formula. Grey-filled circles illustrate range sizes ($n = 120$ species). Credit: Icons, PhyloPic under a Creative Commons license CC0 1.0: *Oceanites oceanicus*, *Procellaria aequinoctialis*, Alexandre Vong; *Pterodroma*, Kimberly Haddrell.

Finally, projected changes in range size depend on a species' ability to keep pace with the local rate of climate change¹⁰. When adaptive and dispersal capacities are sufficient, range expansion is expected to predominate, leading to an overall increase in range size. However,

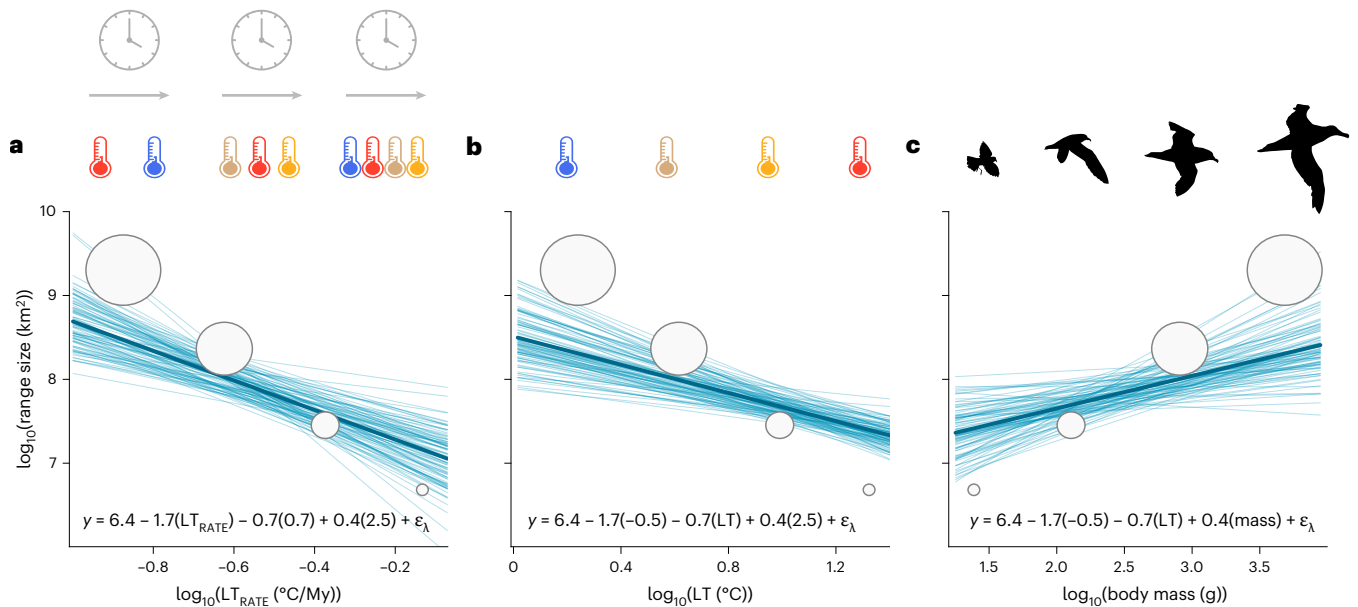


Fig. 3 | Historical range contraction under climate change. **a–c**, The plots show the predicted range size by LT_{RATE} (pMCMC₁₀₀ >95) (**a**), LT (pMCMC₁₀₀ >95) (**b**) and body mass (pMCMC₁₀₀ >95) (**c**). Light-blue lines indicate the posterior regression lines linking body mass with range size. The dark-blue line indicates the mean regression line obtained from the inset model formula. Clocks and thermometers

indicate the rate of LT change. Thermometers indicate the direction of LT change. Grey-filled circles illustrate range sizes. $n = 120$ range size, body mass and LT ; 60,000 LT_{RATE} . Credit: Icons, PhyloPic under a Creative Commons license CC0 1.0: *Oceanites oceanicus*, *Procellaria aequinoctialis*, *Diomedea exulans*, Alexandre Vong; *Pterodroma*, Kimberly Haddrell.

if the rate of climate change exceeds these capacities, as observed in seabirds^{11,12}, local extinctions are expected, resulting in range contraction. We define a species' geographic range following BirdLife International as the geographic extent of suitable habitats occupied during both the non-breeding and breeding seasons (see the Methods for additional criteria).

Here, we evaluated the global seabird responses to historical climate change by reconstructing the historical dispersal routes and LT s of the avian order Procellariiformes, using a posterior sample of phylogenetic trees³⁰ (Extended Data Fig. 2 and Methods). We used the Geo model^{23,25} which allows variation in species dispersal ability as well as continental drift on a spherical space²⁵, explicitly identifying the historical places where seabirds potentially spent most of their lives, that is, the paleo-oceans³¹ (Extended Data Fig. 3). This provides a more realistic recreation of ancestral locations because extant Procellariiformes spend long periods at sea and are therefore effectively pelagic organisms³¹. Using these reconstructions, we inferred the geographic path and distance each species moved across the oceans from the root of the phylogenetic tree to its present location (pathwise distance; Methods). In addition, we extracted simulated palaeotemperatures from the reconstructed locations at phylogenetic nodes (Extended Data Fig. 2 and Methods), allowing us to evaluate the expected effect of climate change on body size, pathwise distance and range size. Finally, to evaluate the extent to which historical inferences align with modern climate change, we applied species distribution models (SDMs) under different warming scenarios projected for 2100, providing holistic insights into global seabird responses to climate change.

Procellariiformes originated in the Australasian seas

Using the maximum clade credibility (MCC) tree of Procellariiformes, the Geo model with variable rates fit the data better than the constant rate model (Bayes factor (BF) >10, very strong support³²), implying that the seabirds' historical geographic expansion was shaped by dispersal at variable rather than constant speeds. The most recent common ancestor (MRCA) of procellariiforms originated in the area encompassing the present-day Coral Sea and the ancient, submerged, Zealandia

continent³³, in the Palaeocene (Fig. 1a), suggesting that the MRCA probably breed and nested along the coast of East Australia and nearby islands. The LT , extracted from the HadCM3 palaeoclimate model and using the MRCA posterior distribution of geographic coordinates (Methods), ranges from 7.9 to 29.5 °C (Fig. 1b), encompassing temperate and tropical temperatures. Finally, when fitting the Geo model on each of the 500 phylogenetic trees, we found consistent results for the MRCA as well as for the main family locations (Extended Data Fig. 4). For example, in over 80% of the 500 analysed trees, we recover the MRCA east offshore Australia (Extended Data Fig. 4a).

Body mass is decoupled from temperature

Using a phylogenetic generalized least squares (PGLS) regression with variable rate (the best fitted model; Extended Data Table 1) and the MCC tree, we modelled body mass as a function of LT , range size, their interaction and the rate of local climate change (LT_{RATE})²⁵, including multiple data per species (Methods). LT_{RATE} quantifies the cumulative change in LT from the common ancestor of seabirds to each extant species, divided by time (Methods) and encompasses both cooling and warming trajectories²⁵. Results show that only range size had a significant positive effect on body mass as 99.6% (>95%) of the estimated coefficients in the posterior distribution crossed zero (pMCMC_{99.6} >95; mean slope of 0.06; Fig. 2), indicating that geographically widespread species tend to be larger. This effect remained significant in over 90% of the regressions performed across 500 phylogenetic trees. Range size overrode the effect of LT on body mass (Extended Data Fig. 1), highlighting the importance of accounting for additional variables when testing the influence of temperature on body mass.

Historical range contraction under climate change

On the basis of a PGLS regression with variable rate (Extended Data Table 1) and using the MCC tree, we predicted range size by LT , LT_{RATE} , body mass, pathwise distance, absolute latitude and an interaction term between pathwise distance and LT_{RATE} . Our results show that only LT , LT_{RATE} and body mass had a significant effect on range size. Warmer LT and higher LT_{RATE} values were associated with smaller

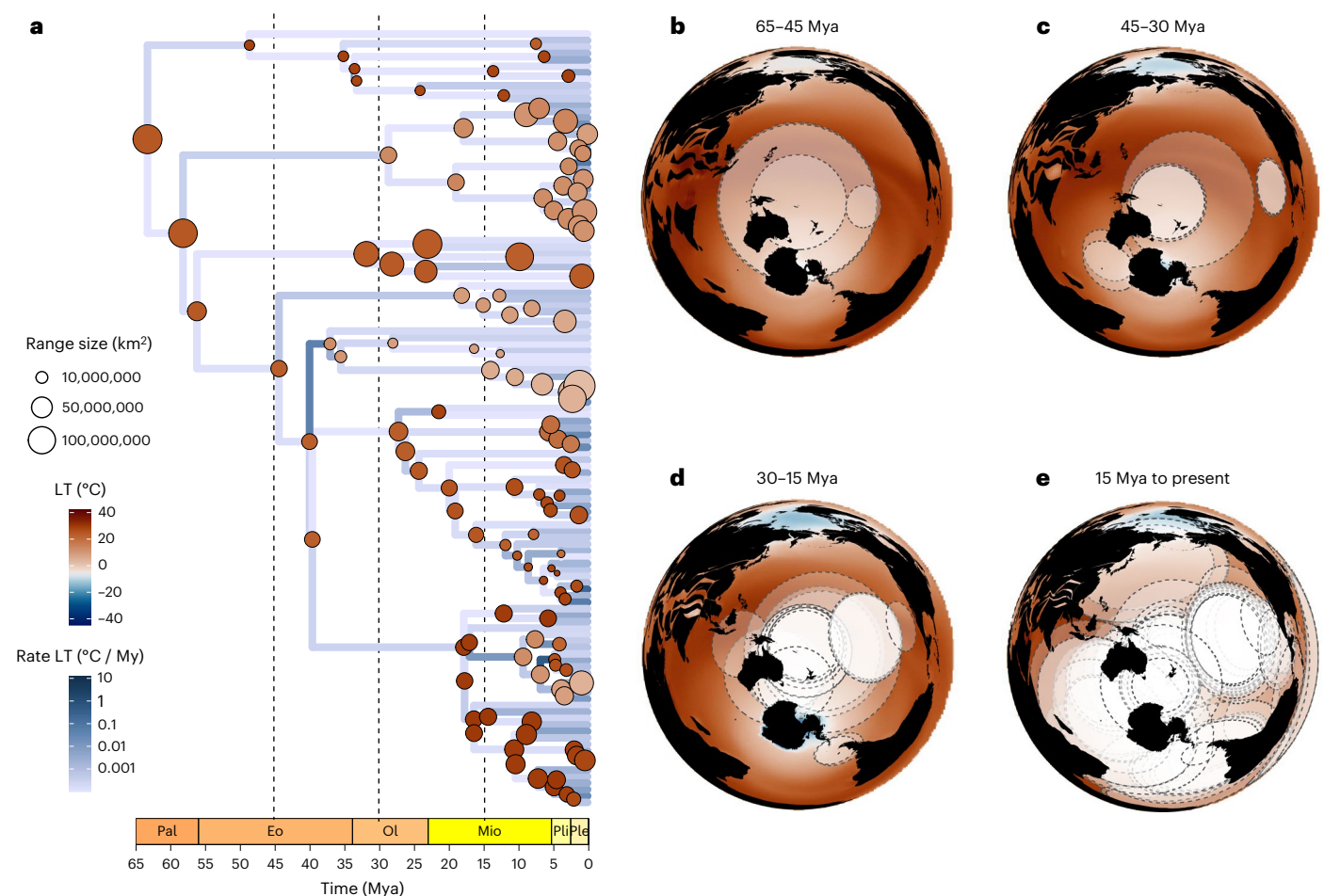


Fig. 4 | Historical range dynamics and species geographic expansion. **a**, Range size (circles at nodes) was modelled as a function of palaeotemperature (LT; coloured circles at nodes) and rate of temperature change (LT_{RATE} ; coloured branches) across the phylogeny. **b–e**, Predicted ancestral range sizes projected onto global palaeomaps for four midtime intervals, shown in

Lambert azimuthal equal-area projection. Maps depict 2-m palaeotemperature, palaeocontinents and node range size, illustrated as transparent circles centred on the node geographic centroid estimated from the Geo model ($n = 120$ species; Supplementary Data File 10 (ref. 38)).

range size (LT mean slope -0.81 , $pMCMC_{100} > 95$; LT_{RATE} mean slope -1.65 , $pMCMC_{100} > 95$; Fig. 3a,b). In addition, body mass was positively associated with range size (mean slope 0.38 , $pMCMC_{100} > 95$; Fig. 3c). Results remain similar when running the PGLS over the sample of 500 trees, suggesting that rapid historical warming reduce seabirds' range size, which might select for smaller sized species. Such range size reduction is probably due to their limited adaptive responses to local climate change^{11,12}.

The variable rate PGLS regression model that considers LT , LT_{RATE} and body mass explained 67% (mean $R^2 = 0.67$) of the variance in range size. When exploring the effect size of each independent variable, we found that LT , LT_{RATE} and body mass explained 1%, 35% and 2% of the variance, respectively (after accounting for shared ancestry). Finally, body mass had a significant and positive effect on range size in 79% of the regression analyses carried out on each of the 500 phylogenetic trees. LT had a negative and significant effect in 100% of the analyses, while LT_{RATE} had a negative and significant effect in 97% of the analyses.

Historical range dynamic and dispersal under climate change

To obtain a general view of historical range dynamic in the face of historical climate change, we predicted ancestral range sizes by integrating the additive effect of LT and LT_{RATE} , while accounting for phylogeny and the Geo model ancestral locations (Fig. 4 and Methods). Originating from an MRCA with a range spanning approximately 125 million km²

(Fig. 4a,b), seabirds predominantly dispersed and diversified across the Pacific Ocean (Fig. 4b–e). Range size reductions were driven by the combined influence of temperature and its rate of change, with change in temperature itself shaped by species dispersal.

On the basis of a PGLS-lambda model (best fitted model; Extended Data Table 1), we predicted pathwise distance by body mass, range size, LT_{RATE} and the interaction between LT_{RATE} and range size. We found a significant effect of range size (mean slope -0.12 , $pMCMC_{98.5} > 95$), LT_{RATE} (mean slope 3.24 , $pMCMC_{100} > 95$) and their interaction (mean slope -0.35 , $pMCMC_{99.9} > 95$; Fig. 5). The negative interaction between LT_{RATE} and range size in predicting pathwise distance suggests that as species are more geographically restricted, they are more sensitive to the rate of local climate change; more rapid climate change increases the selective pressure on dispersal to track suitable habitat elsewhere, as predicted from individual-based model simulations³⁴. The full PGLS model explained 59% of the variance in pathwise distance, with LT_{RATE} and range size accounting for 21% and 1%, respectively. However, the interaction between range size and LT_{RATE} explained 8% of the variance (after accounting for shared ancestry). Finally, the interaction term between range size and LT_{RATE} was negative and significant in 85% of the regression analyses carried out on each of the 500 phylogenetic trees.

On the basis of a Brownian motion PGLS model (best fitted model; Extended Data Table 1), we predicted speciation rate by range size, body

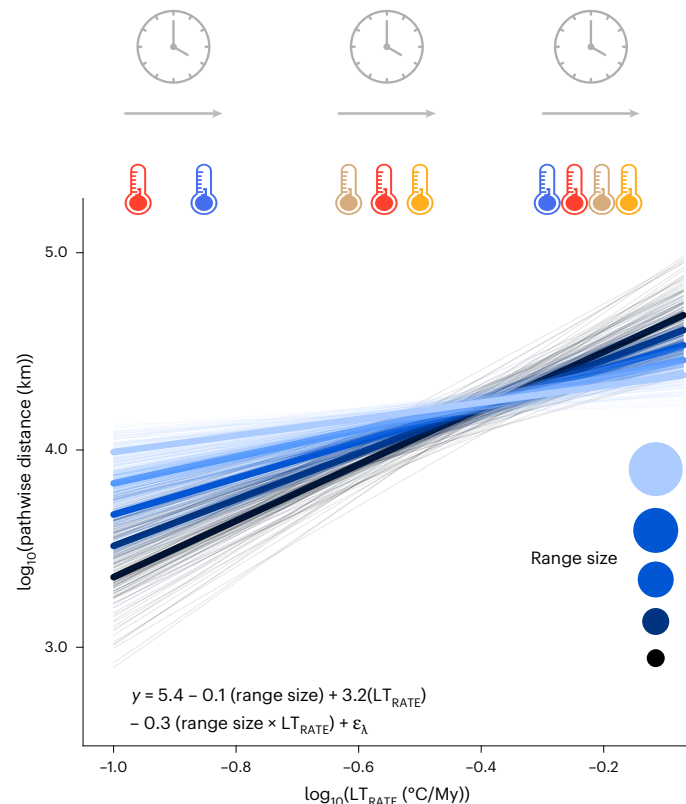


Fig. 5 | Historical range dynamic and dispersal under climate change. The plot shows the predicted pathwise distance by LT_{RATE} (pMCMC₁₀₀ >95), range size (pMCMC_{98.5} >95) and their interaction (pMCMC_{99.9} >95). Light transparent lines indicate the posterior distribution of the regression lines linking pathwise distance with LT_{RATE} across different range size categories. The dark lines indicate the mean regression lines obtained from the inset model formula. Circles represent five different range size categories. Clocks and thermometers indicate the rate of LT change ($n = 120$ range size; 60,000 pathwise distance and LT_{RATE}).

mass, pathwise distance, LT and LT_{RATE} (using samples of trait data; Methods). We found that LT_{RATE} body mass had a positive effect (mean slope 0.04, pMCMC_{97.6} >95; mean slope 0.05, pMCMC_{99.4} >95). The mean R^2 of the full model was 8.9%, with LT_{RATE} and body mass explaining -5.6% and -3.4% of the variance in the full model, respectively. Finally, LT_{RATE} had a positive effect in 89% of the regressions carried out across the 500 phylogenetic trees. However, body mass had a positive effect in 53% of the regressions only, leaving large degrees of uncertainty about its effects on speciation.

Modern range dynamic and dispersal under climate change

To investigate whether the inferred responses in historical time differ from what would be expected today, we carried out SDMs to predict changes in range size and range shifts under a low-rate (Representative Concentration Pathway (RCP) 2.6) and high-rate (RCP 8.5) warming scenario projected by 2100. SDMs show that a higher proportion of species (over 70%) contract their ranges under the high-rate scenario (Fig. 6a and Extended Data Fig. 5). When predicting the range-centroid shift in both scenarios by the percentage of range size change (considering phylogeny and SDM replicates as random effects; Methods), we found that the highest range shifts are predicted under the strongest range contractions in the high-rate scenario only (slope 95% confidence interval (CI), -0.0026 to -0.0011; Fig. 6b). Results from the SDMs align with the historical responses inferred from phylogenetic analyses, demonstrating that range contraction and long-distance dispersal under high rates of climate change are general seabird responses, regardless of timescale.

Discussion

This study suggests that seabirds in the order Procellariiformes historically adapted to rapid change in local climate by contracting their geographic ranges and dispersing longer distances, which contrasts with body mass reductions and dispersal observed in marine ectotherms such as fish. However, as in fish³⁵ and other terrestrial species³⁶, our study shows that seabirds are facing unprecedented rates of climate change. The estimated LT_{RATE} across the phylogenetic branches of the sample of 500 phylogenetic trees, shows that seabirds have historically adapted to a median rate of 2.2×10^{-5} °C per decade, which is approximately four orders of magnitude slower than the current 0.13 °C of warming per decade³⁷. Nevertheless, our million-year historical inferences align with the expected responses under projected scenarios of climate change by 2100, as the SDM models show stronger range contraction and increased range shifts under the highest rate scenario (Fig. 6 and Supplementary Data File 1 (ref. 38)). This consistency across temporal scales supports the idea that our phylogenetic approach can effectively inform species responses to future climate change, despite the unavoidable assumptions and uncertainties that go into modelling the past evolutionary and biogeographic processes.

An important methodological aspect of our study is the extent to which our historical inferences are dependent on the phylogenetic tree used. The phylogeny of the order Procellariiformes is well known for being difficult to reconstruct, with conflicting topologies arising from different sample sizes and genomic markers³⁹. As we are reconstructing palaeoclimate and geographic locations for each phylogenetic node using the Jetz et al. phylogeny³⁰ that has conflicting relationship at deeper nodes, different topologies could dramatically change the results. We addressed this concern by running sensitive analyses using the updated phylogeny of Estandia et al.³⁹ that was reconstructed using molecular data for 51 species³⁹. Results remain similar for ancestral location reconstructed at deeper nodes, including the root and family-level common ancestors, with estimates overlapping those from the 500 posterior trees of Jetz et al. (Extended Data Fig. 4). Similarly, PGLS regressions predicting range size and dispersal distance under rapid local climate change remained consistent (Extended Data Table 2). These findings demonstrate that our conclusions that seabirds contract their geographic ranges and increase dispersal in response to rapid climate change are robust to lower sampling fractions and topological differences. However, the LT_{RATE} metric did not have a significant effect on speciation rates estimated from the Estandia et al. phylogeny (although it was close to the 95% of significance level; mean slope LT_{RATE} 0.08, pMCMC_{93.1} <95; Extended Data Table 2). Thus, conclusions about the effect of LT_{RATE} on seabird speciation rate should be considered with caution. Finally, body mass did not have a significant effect on speciation rate nor was closer to significance when using the phylogeny of Estandia et al., which align with our original results, as body mass was not a significant predictor of speciation rates in 47% of the 500 PGLS regressions.

Another important concern regarding our historical inferences is the absence of fossil data in the Geo model analyses. The inclusion of fossil information close to the origin of a clade (the root of a phylogenetic tree) can drastically change the inference of its geographic location^{40,41}. However, the fossil record of early Procellariiformes is scarce, fragmentary and subject to high degrees of taxonomic uncertainty⁴², which limits our ability to evaluate the robustness of our results to the inclusion of fossils. Despite this, early procellariiforms' fossils tentatively assigned to Diomedidae and Procellariidae, from the late Eocene in the Antarctic Peninsula, align with our inferred locations for those families (Fig. 4 and Extended Data Fig. 4), which suggest that our results may not change drastically with the inclusion of early, taxonomically certain, procellariiforms' fossils. In addition, there were many more Procellariiformes in geographic regions where the climate has historically changed more rapidly, such as the north Atlantic (and other areas). Such observations from the fossil record

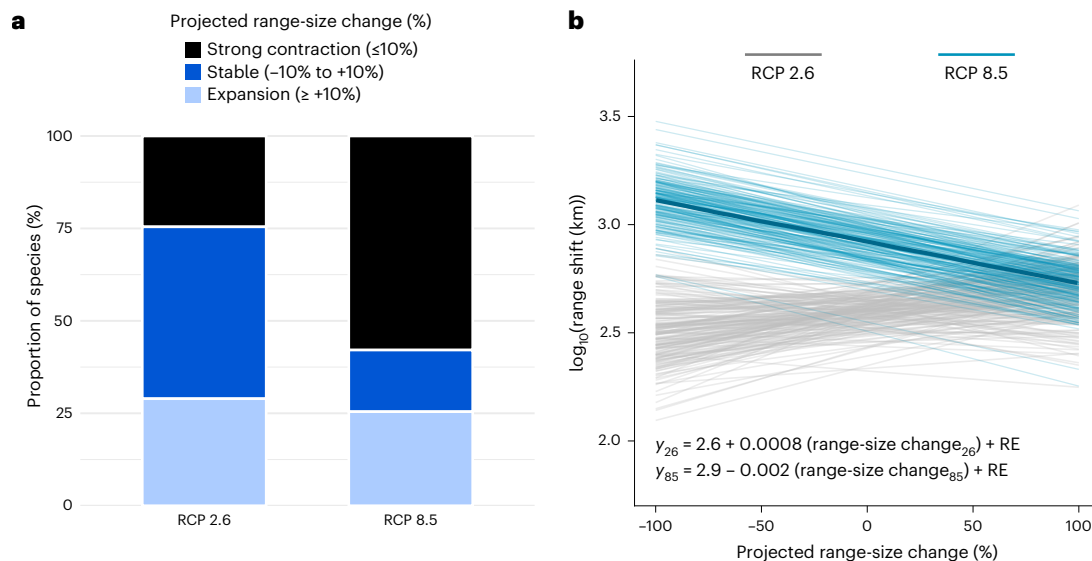


Fig. 6 | Modern range dynamic and dispersal under climate change.

a, Proportion of species that either contract or expand their ranges under the low-rate (RCP 2.6) and high-rate (RCP 8.5) warming scenarios. **b**, Predicted effect of range-size change on range shift under both scenarios, with a significant negative effect on the high-rate scenario only (slope 95% CI, -0.0026 to -0.0011).

Transparent lines indicate the posterior regression lines. Dark line indicates the mean regression line obtained from the inset model formula. RE, random effects including phylogeny and five Species Sensitivity Distribution model replicates ($n = 114$ species with over 50 occurrences).

suggest the fundamental role of climate change in the extinction of Procellariiformes, a role that warrants further study.

Our study emphasizes that the rate of local climate change is far more important than its direction in driving species evolution and in predicting future seabird responses to anthropogenic climate change. This is because LT_{RATE} had the largest effect size in regressions predicting range size, dispersal distance and speciation rate. Notably, SDMs also predict stronger range contractions and longer dispersal distances under the highest rate of projected warming. These results align with recent studies of climate change velocity⁴³ and with the evolutionary theory that first highlighted the importance of rate over direction several decades ago⁴⁴. Therefore, conservation efforts should focus more on how fast the LT changes instead of its direction.

Our results suggest that range dynamics and dispersal responses to climate change should be explicitly incorporated into seabird conservation strategies, with particular emphasis on species with small geographic ranges and limited dispersal capacity. On the basis of our SDMs, we identify four Procellariiformes predicted to face extinction under severe warming scenarios projected for 2100 (Extended Data Fig. 5): the Galápagos Petrel, the Jouanin's Petrel, the Newell's Shearwater and the White-vented Storm Petrel. These findings underscore the urgent need to merge historical insights on dispersal and niche tracking with contemporary projections, so that targeted climate mitigation and marine protection can avert irreversible losses of pelagic biodiversity in a rapidly warming ocean.

Online content

Any methods, additional references, Nature Portfolio reporting summaries, source data, extended data, supplementary information, acknowledgements, peer review information; details of author contributions and competing interests; and statements of data and code availability are available at <https://doi.org/10.1038/s41558-026-02655-4>.

References

- Otero, X. L., De La Peña-Lastra, S., Pérez-Alberti, A., Ferreira, T. O. & Huerta-Díaz, M. A. Seabird colonies as important global drivers in the nitrogen and phosphorus cycles. *Nat. Commun.* **9**, 246 (2018).
- Sydean, W., Thompson, S. & Kitaysky, A. Seabirds and climate change: roadmap for the future. *Mar. Ecol. Prog. Ser.* **454**, 107–117 (2012).
- Jenouvrier, S. Impacts of climate change on avian populations. *Glob. Chang. Biol.* **19**, 2036–2057 (2013).
- Dias, M. P. et al. Threats to seabirds: a global assessment. *Biol. Conserv.* **237**, 525–537 (2019).
- Oro, D. Seabirds and climate: knowledge, pitfalls, and opportunities. *Front. Ecol. Evol.* **2**, 2–79 (2014).
- Orgeret, F. et al. Climate change impacts on seabirds and marine mammals: the importance of study duration, thermal tolerance and generation time. *Ecol. Lett.* **25**, 218–239 (2022).
- Sydean, W. J. et al. Hemispheric asymmetry in ocean change and the productivity of ecosystem sentinels. *Science* **372**, 980–983 (2021).
- He, J., Tu, J., Yu, J. & Jiang, H. A global assessment of Bergmann's rule in mammals and birds. *Glob. Chang. Biol.* **29**, 5199–5210 (2023).
- Bozinovic, F., Calosi, P. & Spicer, J. I. Physiological correlates of geographic range in animals. *Annu. Rev. Ecol. Evol. Syst.* **42**, 155–179 (2011).
- Kerr, J. T. Racing against change: understanding dispersal and persistence to improve species' conservation prospects. *Proc. R. Soc. Lond. B* **287**, 20202061 (2020).
- Boyles, J. G., Seebacher, F., Smit, B. & McKechnie, A. E. Adaptive thermoregulation in endotherms may alter responses to climate change. *Integr. Comp. Biol.* **51**, 676–690 (2011).
- Oswald, S. A. & Arnold, J. M. Direct impacts of climatic warming on heat stress in endothermic species: seabirds as bioindicators of changing thermoregulatory constraints. *Integr. Zool.* **7**, 121–136 (2012).
- Fristoe, T. S. et al. Metabolic heat production and thermal conductance are mass-independent adaptations to thermal environment in birds and mammals. *Proc. Natl Acad. Sci. USA* **112**, 15934–15939 (2015).
- Clarke, A. & Johnston, N. M. Scaling of metabolic rate with body mass and temperature in teleost fish. *J. Anim. Ecol.* **68**, 893–905 (1999).

15. Clarke, A. *Principles of Thermal Ecology. Temperature, Energy and Life* (Oxford Univ. Press, 2017); <https://doi.org/10.1093/oso/9780199551668.001.0001>.
16. Gardner, J. L., Peters, A., Kearney, M. R., Joseph, L. & Heinsohn, R. Declining body size: a third universal response to warming?. *Trends Ecol. Evol.* **26**, 285–291 (2011).
17. Xiong, Y., Fan, L., Chang, Y., Xiao, H. & Lei, F. Warm temperature is associated with reduced body mass and diversification rates while increasing extinction risks in cold-adapted seabirds. *Glob. Chang. Biol.* **30**, 1–11 (2024).
18. Rubenstein, M. A. et al. Climate change and the global redistribution of biodiversity: substantial variation in empirical support for expected range shifts. *Environ. Evid.* **12**, 7 (2023).
19. Comte, L. et al. Bringing traits back into the equation: a roadmap to understand species redistribution. *Glob. Chang. Biol.* **30**, 1–21 (2024).
20. Votier, S. C. & Sherley, R. B. Seabirds. *Curr. Biol.* **27**, R448–R450 (2017).
21. Welch, A. J. et al. Population divergence and gene flow in an endangered and highly mobile seabird. *Heredity* **109**, 19–28 (2012).
22. Lenoir, J. et al. Species better track climate warming in the oceans than on land. *Nat. Ecol. Evol.* **4**, 1044–1059 (2020).
23. O'Donovan, C., Meade, A. & Venditti, C. Dinosaurs reveal the geographical signature of an evolutionary radiation. *Nat. Ecol. Evol.* **2**, 452–458 (2018).
24. Pagel, M., Meade, A. & Barker, D. Bayesian estimation of ancestral character states on phylogenies. *Syst. Biol.* **53**, 673–684 (2004).
25. Avaria-Llautureo, J. et al. The radiation and geographic expansion of primates through diverse climates. *Proc. Natl Acad. Sci. USA* **122**, 1–10 (2025).
26. Claramunt, S., Derryberry, E. P., Remsen, J. V. & Brumfield, R. T. High dispersal ability inhibits speciation in a continental radiation of passerine birds. *Proc. R. Soc. Lond. B* **279**, 1567–1574 (2012).
27. Weeks, B. C. & Claramunt, S. Dispersal has inhibited avian diversification in Australasian archipelagoes. *Proc. R. Soc. Lond. B* **281**, 20141257 (2014).
28. Claramunt, S. et al. A new time tree of birds reveals the interplay between dispersal, geographic range size, and diversification. *Curr. Biol.* **35**, 3883–3895 (2025).
29. Ferrer Obiol, J. et al. Palaeoceanographic changes in the late Pliocene promoted rapid diversification in pelagic seabirds. *J. Biogeogr.* **49**, 171–188 (2022).
30. Jetz, W., Thomas, G. H., Joy, J. B., Hartmann, K. & Mooers, A. O. The global diversity of birds in space and time. *Nature* **491**, 444–448 (2012).
31. Chown, S. L., Gaston, K. J. & Williams, P. H. Global patterns in species richness of pelagic seabirds: the Procellariiformes. *Ecography* **21**, 342–350 (1998).
32. Raftery, A. E. in *Markov Chain Monte Carlo in Practice* (eds Gilks, W., Richardson, S. & Spiegelhalter, D.) 163–187 (Chapman & Hall, 1996).
33. Mortimer, N. et al. Zealandia: Earth's hidden continent. *GSA Today* <https://doi.org/10.1130/GSATG321A.1> (2017).
34. Boeye, J., Travis, J. M. J., Stoks, R. & Bonte, D. More rapid climate change promotes evolutionary rescue through selection for increased dispersal distance. *Evol. Appl.* **6**, 353–364 (2013).
35. Avaria-Llautureo, J. et al. Historical warming consistently decreased size, dispersal and speciation rate of fish. *Nat. Clim. Chang.* **11**, 787–793 (2021).
36. Quintero, I. & Wiens, J. J. Rates of projected climate change dramatically exceed past rates of climatic niche evolution among vertebrate species. *Ecol. Lett.* **16**, 1095–1103 (2013).
37. von Schuckmann, K. et al. *The State of the Global Ocean* (Copernicus Publications, 2024).
38. Avaria-Llautureo, J. et al. Data from: seabird range contraction and dispersal under climate change. *figshare* <https://doi.org/10.6084/m9.figshare.29900165.v1> (2026).
39. Estandía, A. et al. Substitution rate variation in a robust Procellariiform seabird phylogeny is not solely explained by body mass, flight efficiency, population size or life history traits. Preprint at *bioRxiv* <https://doi.org/10.1101/2021.07.27.453752> (2021).
40. Wisniewski, A. L., Lloyd, G. T. & Slater, G. J. Extant species fail to estimate ancestral geographical ranges at older nodes in primate phylogeny. *Proc. R. Soc. Lond. B* **289**, 1–9 (2022).
41. Faurby, S., Silvestro, D., Werdelin, L. & Antonelli, A. Reliable biogeography requires fossils: insights from a new species-level phylogeny of extinct and living carnivores. *Proc. R. Soc. Lond. B* **291**, 1–10 (2024).
42. Acosta Hospitaleche, C. & Gelfo, J. N. Procellariiform remains and a new species from the latest Eocene of Antarctica. *Hist. Biol.* **29**, 755–769 (2017).
43. Loarie, S. R. et al. The velocity of climate change. *Nature* **462**, 1052–1055 (2009).
44. Simpson, G. G. *The Major Features of Evolution* (Columbia Univ. Press, 1953).
45. Valdes, P. J. et al. The BRIDGE HadCM3 family of climate models: HadCM3@Bristol v1.0. *Geosci. Model Dev.* **10**, 3715–3743 (2017).

Publisher's note Springer Nature remains neutral with regard to jurisdictional claims in published maps and institutional affiliations.

Open Access This article is licensed under a Creative Commons Attribution 4.0 International License, which permits use, sharing, adaptation, distribution and reproduction in any medium or format, as long as you give appropriate credit to the original author(s) and the source, provide a link to the Creative Commons licence, and indicate if changes were made. The images or other third party material in this article are included in the article's Creative Commons licence, unless indicated otherwise in a credit line to the material. If material is not included in the article's Creative Commons licence and your intended use is not permitted by statutory regulation or exceeds the permitted use, you will need to obtain permission directly from the copyright holder. To view a copy of this licence, visit <http://creativecommons.org/licenses/by/4.0/>.

© The Author(s) 2026

Methods

Phylogenetic trees

We obtained a Bayesian sample of 500 phylogenetic trees for 121 species of Procellariiformes (Hackett source) from BirdTree³⁰. We excluded the Jamaican Petrel (*Pterodroma caribbaea*) because its International Union for Conservation of Nature (IUCN) status is 'possibly extinct'. The phylogenetic uncertainty associated to divergence time (branch lengths) and topology can be found graphically as a DensiTree (Extended Data Fig. 2). We obtained an MCC tree by applying the maxCladeCred function of the phangorn R-package version 2.12.1⁴⁶ on the sample containing 9,993 avian species.

Species body mass and geographic range size

We obtained species body mass (in grams) from the AVONET database⁴⁷. Species range size was obtained from the species geographic distribution polygons available in the BirdLife International database⁴⁸ (accessed on 8 February 2024). To get the polygons range size, we calculated their area in square kilometres using the area function of the raster R-package, version 3.6-30⁴⁹. Most of the estimated areas were identical to the area available in the AVONET database. However, there were approximately ten species for which the AVONET data showed over- and underestimation of the range area, probably owing to the use of an older version of the polygon database. The polygon areas are available in Supplementary Data File 2 (ref. 38).

Species geographic distribution data

We generated geographic coordinates (longitude and latitude) within the BirdLife polygons⁴⁸, which represent the best available estimates of avian geographic ranges based on expert contributions, observational data and rigorous validation criteria. The full list of criteria used to construct the geographic distribution polygons is as follows:

- (1) The species is known or thought very likely to occur currently in the area, which encompasses localities with current or recent (last 20–30 years) records where a suitable habitat at appropriate altitudes remains.
- (2) The species is/was native to the area.
- (3) The species is/was known or thought very likely to be resident throughout the year.
- (4) The species is/was known or thought very likely to occur regularly during the breeding season and to breed and be capable of breeding.
- (5) The species is/was known or thought very likely to occur regularly during the non-breeding season. In the Eurasian and North American contexts, this encompasses 'winter'.

These polygons help mitigate biases associated with undersampled observations, particularly for highly mobile seabirds, by providing robust estimates of their likely geographic extents. The BirdLife database contains current best approximation of the species extent of species, which implicitly assumes inherent uncertainties.

Geographic coordinates were generated randomly within each BirdLife polygon, with the number of random points scaled according to polygon area. Specifically, we generated 50, 100, 200, 300, 400 or 500 random coordinates for polygons with areas of 20–100,000 km², 100,000–200,000 km², 200,000–300,000 km², 300,000–400,000 km², 400,000–500,000 km² and >500,000 km², respectively. This approach allowed us to get a more exhaustive representation of the extent of the species' geographic distribution in comparison with approaches that rely on the observed geographic occurrences or the distribution centroids. Samples of coordinates are plotted, as shown in Extended Data Fig. 3, and are available in Supplementary Data File 3 (ref. 38).

Species ancestral locations

To obtain the location of ancestral Procellariiform species, we applied the Geo model with map restrictions in BayesTraits v5^{23,25}. The Geo

model²³ reconstructs the posterior distribution of longitude and latitude onto a three-dimensional Cartesian coordinates system (x , y and z), so that the model assumes that species change their locations as a moving point in a spherical space. It estimates the posterior distribution of ancestral coordinates at phylogenetic nodes while sampling across all the geographic coordinates for phylogenetic tips (the sample of coordinates within the distribution polygons in this case)—thus considering irregular and patchy nature of species' geographic distribution. The sampling of coordinates data is simultaneously integrated with the estimation of model parameters. Coordinate changes along the branches of the phylogenetic tree—that is, species dispersal—are modelled using Brownian motion, assuming constant dispersal speeds. However, the Geo model accounts for variation in species dispersal speed across phylogenetic branches by means of the variable rate model⁵⁰.

For this study, we used an updated version of the Geo model²⁵ to reconstruct locations to points found only on the world's palaeoceans. Initially, reconstructed locations are placed on oceans; when proposing a new location, the closest point to the proposed location is identified on the map. If the closest point is found to be on the land, the new location is assigned as zero probability (rejected), otherwise it is accepted or rejected on the basis of its likelihood. Geography is not static through time, and palaeomaps were created for different time periods. As the phylogeny is time calibrated, each internal node is assigned a palaeomap on the basis of its age, ensuring that the reconstructed longitudes and latitudes for the phylogenetic internal nodes (that, is ancestral species) remained within the boundaries of the ancestral ocean configurations, thus, accounting explicitly for continental drift. To restrict the space for ancestral location inferences across phylogenetic nodes, we used the global maps of the PALEOMAP project⁵¹, generated with the rgplates R-package, version 0.6.1^{32,53}. The PALEOMAP project contains global maps for every million years, during the past 1,100 million years.

We ran ten MCMC chains for the Geo model with map restrictions, 400,000,000 million iterations each, discarding the first 300,000,000 million iterations as burn-in and sampling every 200,000 iterations. We used a uniform prior ranging from 0 to 1,000,000 for the dispersal background variance. These settings gave us a final sample of 500 posterior coordinates per phylogenetic node (Supplementary Data File 4 (ref. 38)). We compared the constant and variable speed models by means of BF. The BF takes the model marginal likelihood for comparison, which is estimated by the steppingstone sampling in BayesTraits⁵⁴. BF is calculated as the double of the difference between the log marginal likelihood of two models. Higher values of the log marginal likelihood represent better-fitted models. By convention, BF > 2 indicates positive support, BF = 5–10 indicates strong support and BF > 10 is considered very strong support for a model over the other³².

Species dispersal ability (pathwise distance)

Having the reconstructed locations across all phylogenetic nodes, we estimated the branchwise distance, which is a measure of the geographic distance that each ancestral species has moved across phylogenetic branches^{23,35}. We calculated the branchwise distance using the Great Circle distance, which is the shortest geographic distance between two geographic points on a spherical surface. As geographic points linked to each branch, we used each coordinate from the posterior distribution of 500 coordinates per phylogenetic node.

We summed the branchwise distances along the paths that link the common ancestor of Procellariiformes with each extant species. This variable, the pathwise distance^{23,35}, allows us to have a measure of the geographic distance that each extant species has moved over the globe since and from the origin of the common ancestor. As we have 500 data points of branchwise distance, then we obtained a final dataset of 500 pathwise distances for each species. In this way, we can include the uncertainty in the ancestral location estimation when estimating the pathwise distance. These data are available in Supplementary Data File 5 (ref. 38).

The pathwise distance effectively brings a measure of the variability in species dispersal capacity inferred for Procellariiformes, during the last ~63 million years of evolution. Interestingly, the pathwise distance neither correlates with the commonly used indirect metric of birds' dispersal ability—the hand–wind index^{14,15}—nor the wing length (Extended Data Fig. 6). This lack of association suggests that the hand–wind index and wing length do not represent the distances that procellariiform species have dispersed over evolutionary time, potentially because there are other flight methods, such as dynamic soaring, that might be more relevant for species dispersal capacity.

Extant species temperature data (LT)

We extracted present-day sea surface temperature (SST) from the Bio-ORACLE database⁵⁵ by means of the geodata R package, version 0.6-2⁵⁶. We extracted the SST from the within-polygon sample of coordinates so that we can capture the full intraspecific variation in temperature to which each species is adapted in the present (Supplementary Data File 3 (ref. 38)). We used SST for two reasons. First, SST is the most widely used climatic variable in studies of seabird responses to climate change^{2,5,6}, as it integrates environmental conditions across marine ecosystems. Second, as top marine predators, Procellariiformes are highly sensitive to SST changes, which influence prey availability and marine ecosystem dynamics, thereby shaping their distribution and ecological responses^{57,58}. Given that the SST is related to the species' geographic distribution, we called this variable the local sea surface temperature (LT).

Ancestral species palaeotemperature data

For phylogenetic nodes, we extracted the palaeoclimate data from the posterior distribution of coordinates inferred with the Geo model with palaeomap restrictions (Supplementary Data File 4 (ref. 38)). This variable allows us to approximate the local thermal conditions to which ancestral species were adapted²⁵. We obtained the annual mean 2-m palaeotemperature from world palaeoclimate simulations on the basis of the Hadley Centre general circulation Coupled Model (the HadCM3BL-M2.1aD model)^{45,59–61}. The performance of the HadCM3BL-M2.1aD in simulating modern climate is comparable to the Coupled Model Intercomparison Project 5 and 6, state-of-the-art models^{45,61}. Most importantly for our objectives, the HadCM3BL-M2.1aD also recovers the pattern of global temperature change during the last 65 million years as expressed from fossil benthic foraminifera⁶². General circulation models such as the HadCM3BL-M2.1aD have been widely used in current palaeoclimate research that have brought meaningful inferences about palaeoclimate and diversity. Some examples include the FOAM and CESM models^{63–67}.

We used 17 dated-palaeoclimate layers, covering the evolutionary history of Procellariiformes as obtained from the sample of 500 phylogenetic trees. The ages for the climatic layers are as follows (million years ago): 0, 4, 10, 14, 19, 25, 31, 35, 39, 44, 52, 55, 60, 66, 69, 75 and 80 (Extended Data Fig. 2). To extract the palaeotemperature values for the nodes, we used the closest climatic layer to each node given their ages. Of the 119 phylogenetic nodes, 94 (79%) had ages that matched the available palaeoclimatic layers within 2 million years, while the remaining 25 nodes (21%) differed by more than 2 million years. To account for the potential bias introduced by these age differences in the 21% of nodes, we extracted the palaeotemperature from the sample of 500 phylogenetic trees that contains a variation in node ages. In this approach, we can include the node age uncertainty when estimating ancestral species' environmental temperature (Extended Data Fig. 2; see the 'Sensitivity analyses' subheading in the Methods section).

Species rate of local climate change (LT_{RATE})

To obtain a measure of the rate at which the species' environmental temperature has changed during historical time, we used the Pathwise Rate of Local Temperature Change metric (LT_{RATE}; Supplementary

Data File 5 (ref. 38)). This metric was originally implemented in the context of continental temperature change²⁵. The LT_{RATE} was obtained in a three-step approach²⁵. First, we extracted the LT for each phylogenetic node in the tree, using the posterior distribution of geographic coordinates for each node. The posterior distribution of geographic coordinates corresponds to the data obtained with the Geo model. Second, we calculated the palaeo-LT absolute difference between the ancestral and descendant nodes per phylogenetic branch. Third, we summed all the per-branch absolute differences of LT, along the paths that link the common ancestor with each extant species, and we divided this variable by the total time of each path given the tree. Crucially, LT_{RATE} represents non-directional changes, that is, changes can be to either cooler or warmer waters. LT_{RATE} gives us an estimation of the rate of change in LT. We also estimated the LT_{RATE} using the posterior distribution of 500 coordinates inferred with the Geo model. Therefore, we obtained a dataset of 500 LT_{RATE} for each species given the MCC tree. Finally, we also estimated the LT_{RATE} using the sample of 500 phylogenetic tree to include the node age uncertainty in our downstream analyses.

Speciation rate

To study the correlates of speciation rates, we used the node count (NC) along phylogenetic paths (Supplementary Data File 5 (ref. 38)). There are alternative non-model-based tip-rate metrics used to study the speciation rate correlates, such as the inverse of equal splits or the inverse of terminal branch length⁶⁸. NC captures the average speciation rate over the entire phylogenetic path and weight equally all branch lengths along the paths. We did not use a tip-rate speciation metric estimated from time-varying birth–death diversification models such as BAMM⁶⁸, as the tip-rates metric is more suitable to study speciation in recent times (not in deep time as in our study). In addition, it has also been shown in the context of phylogenetic regressions that NC is the response variable that exhibits the highest statistical power when compared with regressions using equal splits or terminal branch length as speciation metrics⁶⁹.

Phylogenetic regressions

We conducted Bayesian phylogenetic regression analyses in BayesTraits v5. We tested for multiple evolutionary models that can fit the regression residual variance, that is, the Brownian motion model, the lambda model, the Ornstein–Uhlenbeck model, the variable rate model and a combination of the lambda and variable rate model⁷⁰. We ran PGLS regressions using body mass, range size, pathwise distance and speciation rate as response variables. For each response variable, we evaluated the influence of several predictors that has been proposed to correlate with each response variable (Supplementary Methods).

We used samples of trait data in our Bayesian PGLS, which allows us to consider within-species variation in the traits of interest. Traditionally comparative methods assume trait values are known without error, but traits often show within-species variation. BayesTraits allows samples of data to be used. The estimation of both the regression parameters and the evolutionary model parameters are integrated over the sample of trait data⁷¹. The Markov chain explores the samples of trait data across iterations, accepting or rejecting them on the basis of its likelihood. We used the samples of trait data for the LT data as obtained from the coordinates generated at random within the BirdLife polygons ($n \approx 500$ per species), pathwise distance ($n = 500$ per species) and LT_{RATE} ($n = 500$ per species).

We estimated the effect size of each predictor variable by taking the difference of the R^2 values between the regression with all the significant predictors and without the predictor of interest. We ran PGLS multiple regressions under Brownian motion and using the branch-scaled phylogenetic tree obtained from the PGLS with variable rate. We conducted PGLSs under Brownian motion and using the scaled tree to stabilize the inferred background variance when estimating the effect size of each predictor.

We did not use other regression approaches that examine and quantify the direct and indirect relationships between variables, such as phylogenetic path analyses, because those approaches can neither fit variable rate models nor consider the intraspecific variation in the data when estimating regression parameters as BayesTraits does. We rather evaluated the effect of the hypothesized covariates for each response variables, and we also tested for interactions between covariates when they were expected to be associated given previous hypotheses. Please see the Supplementary Methods for a detailed explanation of each regression model formulation.

Finally, regression coefficients were considered to have a significant effect on the response variable on the basis of a calculated value of pMCMC for each of their posterior distribution. When >95% of the estimated coefficients in the posterior distribution crossed zero, this indicate that the coefficient is significantly different from zero.

Phylogenetic prediction of ancestral range size

To better understand the evolution of range size under historical climate change, we conducted a phylogenetic predictive approach to estimate unknown values of range size at phylogenetic nodes following the approach in refs. 71,72. We based our phylogenetic prediction on the PGLS regression model with variable rate so that we can account for the variation in the rate of range size evolution when estimating ancestral states (model comparison showed that the variable rate model fit the data better than other evolution models). We ran the PGLS regression with variable rate in BayesTraits, using the known values of range size as response variable and the known values of LT and LT_{RATE} as predictors (as we found those predictors to be significant in our regression models; see the ‘Historical range contraction under climate change’ section). Then, we estimated the maximum likelihood unknown values of range size at each ‘false tip’ on the basis of the ‘known’ values of LT and LT_{RATE} at each phylogenetic node. These known values of LT and LT_{RATE} at phylogenetic nodes were estimated on the basis of both the node location that were obtained from the Geo model with map restrictions and the palaeoclimate simulation.

Sensitivity analyses

We tested the robustness of all our results to the phylogenetic uncertainty of Procellariiformes in terms of divergence times (branch lengths) and topological structure by conducting all our analyses on two phylogenies—the posterior sample of 500 phylogenetic trees obtained from Jetz et al.³⁰ and the MCC tree of Estandia et al.³⁹ The phylogeny of Estandia et al. was reconstructed for 51 species with molecular data that shows contrasting topologies at deeper, family-level nodes.

We ran the Geo model with map restrictions across each of the 500 phylogenetic trees in the posterior distribution. Then, we obtained the posterior distribution of species pathwise distance from each of these 500 Geo model analyses ($n = 500$ pathwise distance from each of the 500 trees). We also obtained the LT at phylogenetic nodes, and the LT_{RATE} metric, from each of the 500 phylogenetic trees ($n = 500$ LT and LT_{RATE} , from each of the 500 trees). The node ancestral locations, node palaeotemperature and pathwise metrics obtained from each of the 500 phylogenetic trees of Jetz et al. are available in Supplementary Data Files 6 and 7 (ref. 38).

We evaluated the effect of phylogenetic uncertainty across all the final PGLS regressions models for each response variable. The final regression models were those regression models that have the statistically significant predictors only, using the MCC tree. Then, we ran the PGLS regression models across each of the 500 phylogenetic trees in BayesTraits v5, using samples of trait data. This means that, for each of the 500 PGLS, we used samples of trait data for LT ($n \approx 500$ per species), LT_{RATE} ($n = 500$ per species) and pathwise distance ($n = 500$ per species). We also used samples of trait data for the interacting terms between predictors, when necessary. Finally, we conducted all those analyses using the phylogeny of Estandia et al.³⁹

SDMs

To estimate the extant spatial distribution of seabirds, we carried out SDMs using at least 50 occurrences per species that were obtained from the GBIF database (Supplementary Data File 8 (ref. 38)) and environmental data from the Bio-ORACLE v2.2 database with a spatial resolution of 9.2 km (ref. 73). We obtained the occurrences using the `occ_search()` function of the `rgbifR` package. Environmental predictors included SST-derived variables (annual mean, minimum and maximum; long-term minimum and maximum; and range). To mitigate collinearity, we applied principal component analysis, retaining the first two principal components, which accounted for 99% of the variance. For each species, pseudo-absences were generated within a 600-km radius around presence records, matching the number of absences to presences. This buffer zone is close to the median foraging range (approximately 607 km) obtained across multiple flying seabirds⁷⁴. Data were partitioned into four spatial subsets for training and testing, and random forest models were used for modelling. We evaluated model performance using the area under the curve on test data, with values approaching 1 indicating superior fit. We replicated the analyses five times for each species to deal with the stochasticity introduced by the selection of random pseudo-absences.

To project future species distribution, we established a 1,000-km buffer around current presence records, assuming future range shifts would not exceed this radius. This is a reasonable assumption given estimates of species displacement rates of approximately 6 km per decade under current climate change. We projected future species distribution under two RCP scenarios that model future climate scenarios on the basis of greenhouse gas emissions and radiative forcing levels. These scenarios, developed for the Intergovernmental Panel on Climate Change (IPCC), represent different trajectories of emissions and societal responses up to 2100. We used the low-emissions scenario (RCP 2.6) and high-emissions scenario (RCP 8.5), which mainly differ in the rate of climate change. The RCP 2.6 (‘best-case scenario’) projects a global temperature increase of approximately 1.0–1.8 °C by 2100, with a best estimate of -1.5 °C. The RCP 8.5 (‘worst-case scenario’) projects a temperature increase of approximately 3.2–5.4 °C by 2100, with a best estimate of -4.3 °C.

Model probability maps were converted to binary presence–absence maps using analytically determined species-specific thresholds. We estimated the area of occupancy for each species under present and future scenarios, calculating the percentage of range change. Finally, we estimated the distance (in kilometres) of species range shift in each future scenario by calculating the great circle distance between geographic centroids.

Multiresponse phylogenetic mixed models

We fitted multiresponse phylogenetic mixed models using the ‘brms’ R package⁷⁵. As response variables, we used the species range shifts obtained from the SDMs under both the RCP 2.6 and RCP 8.5 scenarios and we used a Gaussian link function with the fixed effect. As fixed effect, we included the percentage of range change under both scenarios. We also included two random effects in the model, the phylogenetic relationships of Procellariiformes and the within-species five SDM replicates, estimating the correlation between residuals. Finally, we used weakly informative priors, running 4,000 MCMC interactions, with 1,500 iterations as warm-up, and sampling every 100 iterations. Model fitting was checked by ensuring Rhats closer to 1 and ESS over 1,000 for the estimated model parameters.

Reporting summary

Further information on research design is available in the Nature Portfolio Reporting Summary linked to this article.

Data availability

All data analysed and outputs from this study are available as Supplementary Data Files 1–10 via figshare at <https://doi.org/10.6084/m9.figshare.29900165> (ref. 38).

Code availability

BayesTraits version 5 is available at <https://www.evolution.reading.ac.uk/BayesTraitsV5.0.3/BayesTraitsV5.0.3.html>. Source code is available via GitHub at <https://github.com/AndrewPMeade/BayesTraits-Release/tree/Release/src>.

References

46. Schliep, K. P. phangorn: phylogenetic analysis in R. *Bioinformatics* **27**, 592–593 (2011).
47. Tobias, J. A. et al. AVONET: morphological, ecological and geographical data for all birds. *Ecol. Lett.* **25**, 581–597 (2022).
48. Bird species distribution maps of the world. Version 2023.1. *BirdLife DataZone* <https://datazone.birdlife.org/species/requestdis> (BirdLife International, 2023).
49. Hijmans, R. raster: Geographic data analysis and modeling. CRAN <https://doi.org/10.32614/CRAN.package.raster> (2024).
50. Venditti, C., Meade, A. & Pagel, M. Multiple routes to mammalian diversity. *Nature* **479**, 393–396 (2011).
51. Scotese, C. R. & Wright, N. PALEOMAP Paleodigital Elevation Models (PaleoDEMS) for the Phanerozoic. *EarthByte* <https://www.earthbyte.org/paleodem-resource-scotese-and-wright-2018/> (2018).
52. Kocsis, A. T., Raja, N. B., Williams, S. & Dowding, E. M. rgplates: R interface for the GPlates Web Service and Desktop Application. *Zenodo* <https://zenodo.org/doi/10.5281/zenodo.8093990> (2024).
53. Müller, R. D. et al. GPlates: building a virtual earth through deep time. *Geochem. Geophys. Geosyst.* **19**, 2243–2261 (2018).
54. Xie, W., Lewis, P. O., Fan, Y., Kuo, L. & Chen, M. H. Improving marginal likelihood estimation for Bayesian phylogenetic model selection. *Syst. Biol.* **60**, 150–160 (2011).
55. Tyberghein, L. et al. Bio-ORACLE: a global environmental dataset for marine species distribution modelling. *Glob. Ecol. Biogeogr.* **21**, 272–281 (2012).
56. Hijmans, R. J., Barbosa, M., Ghosh, A. & Mandel, A. geodata: Access geographic data. CRAN <https://doi.org/10.32614/CRAN.package.geodata> (2024).
57. Quillfeldt, P. & Masello, J. F. Impacts of climate variation and potential effects of climate change on South American seabirds – A review. *Mar. Biol. Res.* **9**, 337–357 (2013).
58. Torres, L. et al. Sea surface temperature, rather than land mass or geographic distance, may drive genetic differentiation in a species complex of highly dispersive seabirds. *Ecol. Evol.* **11**, 14960–14976 (2021).
59. Pope, V. D., Gallani, M. L., Rowntree, P. R. & Stratton, R. A. The impact of new physical parametrizations in the Hadley Centre climate model: HadAM3. *Clim. Dyn.* **16**, 123–146 (2000).
60. Gordon, C. et al. The simulation of SST, sea ice extents and ocean heat transports in a version of the Hadley Centre coupled model without flux adjustments. *Clim. Dyn.* **16**, 16–147 (2000).
61. Valdes, P. J., Scotese, C. R. & Lunt, D. J. Deep ocean temperatures through time. *Clim. Past* **17**, 1483–1506 (2021).
62. Zachos, J., Pagani, H., Sloan, L., Thomas, E. & Billups, K. Trends, rhythms, and aberrations in global climate 65 Ma to present. *Science* **292**, 686–693 (2001).
63. Pohl, A., Wong Hearing, T., Franc, A., Sepulchre, P. & Scotese, C. R. Dataset of Phanerozoic continental climate and Köppen–Geiger climate classes. *Data Brief* **43**, 108424 (2022).
64. Korasidis, V. A., Wing, S. L., Shields, C. A. & Kiehl, J. T. Global changes in terrestrial vegetation and continental climate during the Paleocene–Eocene thermal maximum. *Paleoceanogr. Paleoclimatol.* **37**, 1–21 (2022).
65. Wong Hearing, T. W. et al. Quantitative comparison of geological data and model simulations constrains early Cambrian geography and climate. *Nat. Commun.* **12**, 3868 (2021).
66. Ontiveros, D. E. et al. Impact of global climate cooling on Ordovician marine biodiversity. *Nat. Commun.* **14**, 6098 (2023).
67. Wilson, L. N. et al. Global latitudinal gradients and the evolution of body size in dinosaurs and mammals. *Nat. Commun.* **15**, 2864 (2024).
68. Title, P. O. & Rabosky, D. L. Tip rates, phylogenies and diversification: what are we estimating, and how good are the estimates?. *Methods Ecol. Evol.* **10**, 821–834 (2019).
69. Harvey, M. G. & Rabosky, D. L. Continuous traits and speciation rates: alternatives to state-dependent diversification models. *Methods Ecol. Evol.* **9**, 984–993 (2018).
70. Baker, J., Meade, A., Pagel, M. & Venditti, C. Positive phenotypic selection inferred from phylogenies. *Biol. J. Linnean Soc.* **118**, 95–115 (2016).
71. Organ, C. L., Shedlock, A. M., Meade, A., Pagel, M. & Edwards, S. V. Origin of avian genome size and structure in non-avian dinosaurs. *Nature* **446**, 180–184 (2007).
72. Baker, J., Meade, A., Pagel, M. & Venditti, C. Adaptive evolution toward larger size in mammals. *Proc. Natl Acad. Sci. USA* **112**, 5093–5098 (2015).
73. Assis, J. et al. Bio-ORACLE v2.0: extending marine data layers for bioclimatic modelling. *Glob. Ecol. Biogeogr.* **27**, 277–284 (2018).
74. Weimerskirch, H. Are seabirds foraging for unpredictable resources?. *Deep Sea Res. 2* **54**, 211–223 (2007).
75. Bürkner, P.-C. brms: An R package for Bayesian multilevel models using Stan. *J. Stat. Softw.* **80**, 1–28 (2017).

Acknowledgements

This work was supported by The Center for Ecology and Sustainable Management of Oceanic Islands ESMOI (to G.L.-J.), ANID-ATE grant no. 220044 BioDUCCT (to G.L.-J. and J.A.-L.), ANID/Centros Regionales grant no. R20F0008 (CLAP, to M.M.R.), ANID/FONDECYT grant no. 1251475 (to M.M.R.) and by the Leverhulme Trust Research Leadership Award, grant no. RL-2019-012 (to C.V.).

Author contributions

J.A.-L. conducted a comprehensive literature review, identified key knowledge gaps regarding seabird responses to climate change, developed the methodological framework and led the interpretation of results, figure creation and manuscript writing. M.M.R. performed the species distribution modelling and contributed literature. C.V. provided analytical insights for hypothesis testing and figure presentation. G.L.-J. contributed literature and essential knowledge about seabird natural history. All authors contributed to writing the manuscript and approved the final version.

Competing interests

The authors declare no competing interests.

Additional information

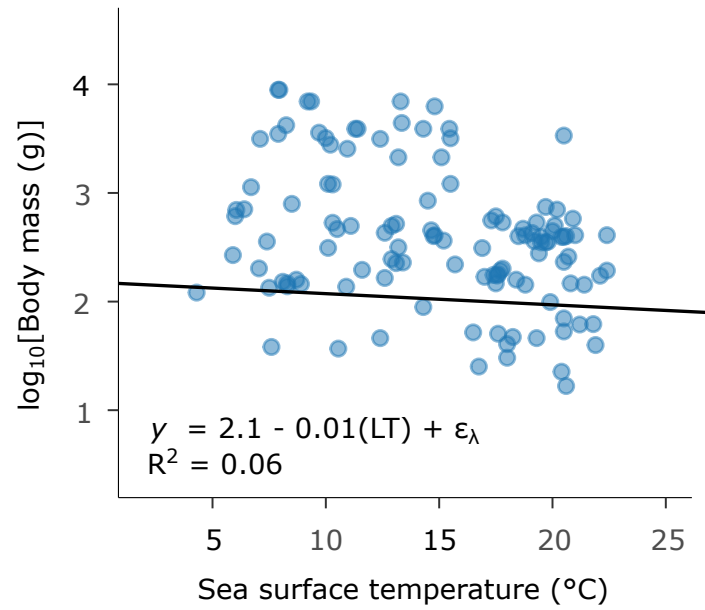
Extended data is available for this paper at <https://doi.org/10.1038/s41558-026-02655-4>.

Supplementary information The online version contains supplementary material available at <https://doi.org/10.1038/s41558-026-02655-4>.

Correspondence and requests for materials should be addressed to Jorge Avaria-Llautureo or Guillermo Luna-Jorquera.

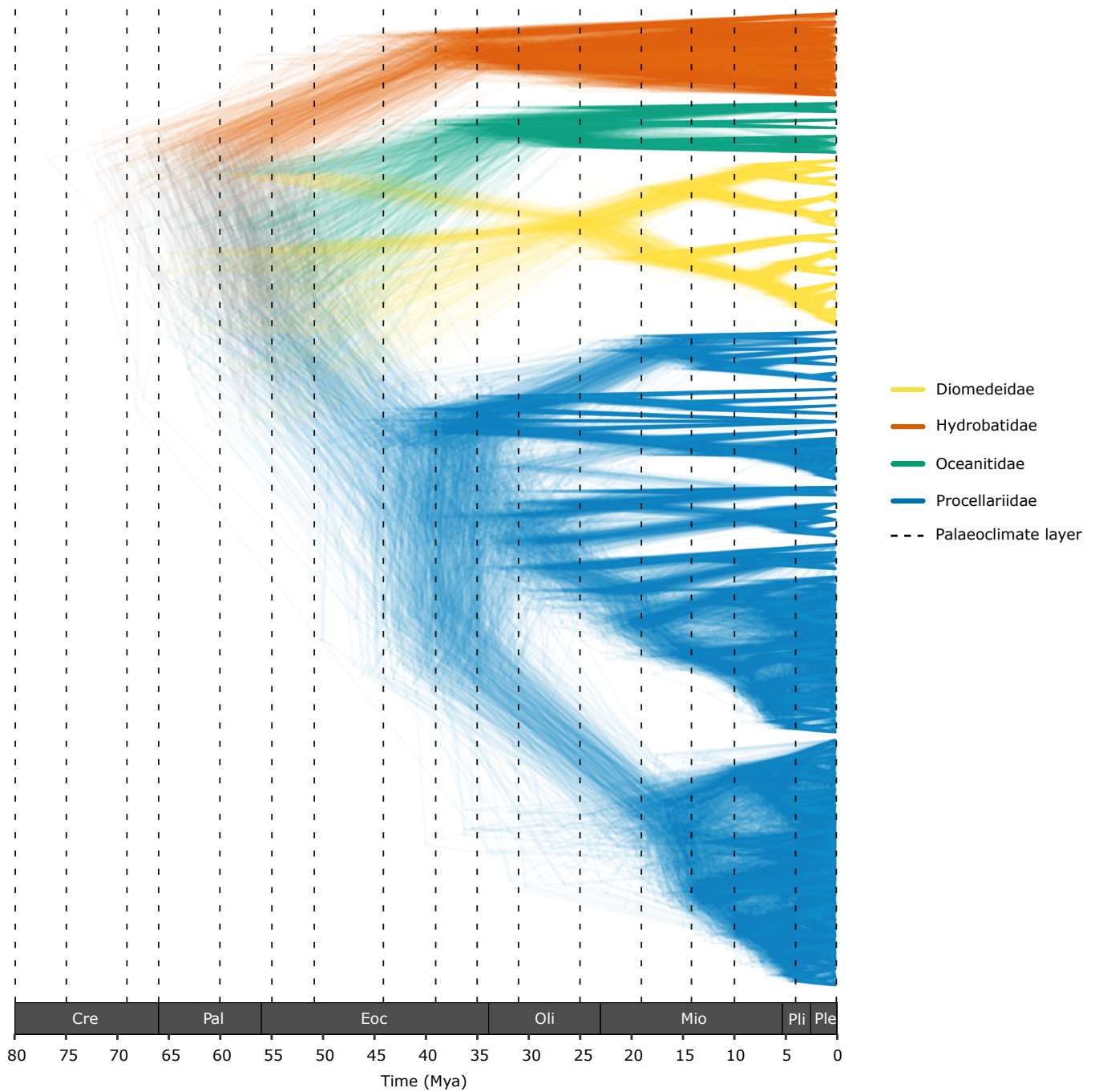
Peer review information *Nature Climate Change* thanks the anonymous reviewer(s) for their contribution to the peer review of this work.

Reprints and permissions information is available at www.nature.com/reprints.



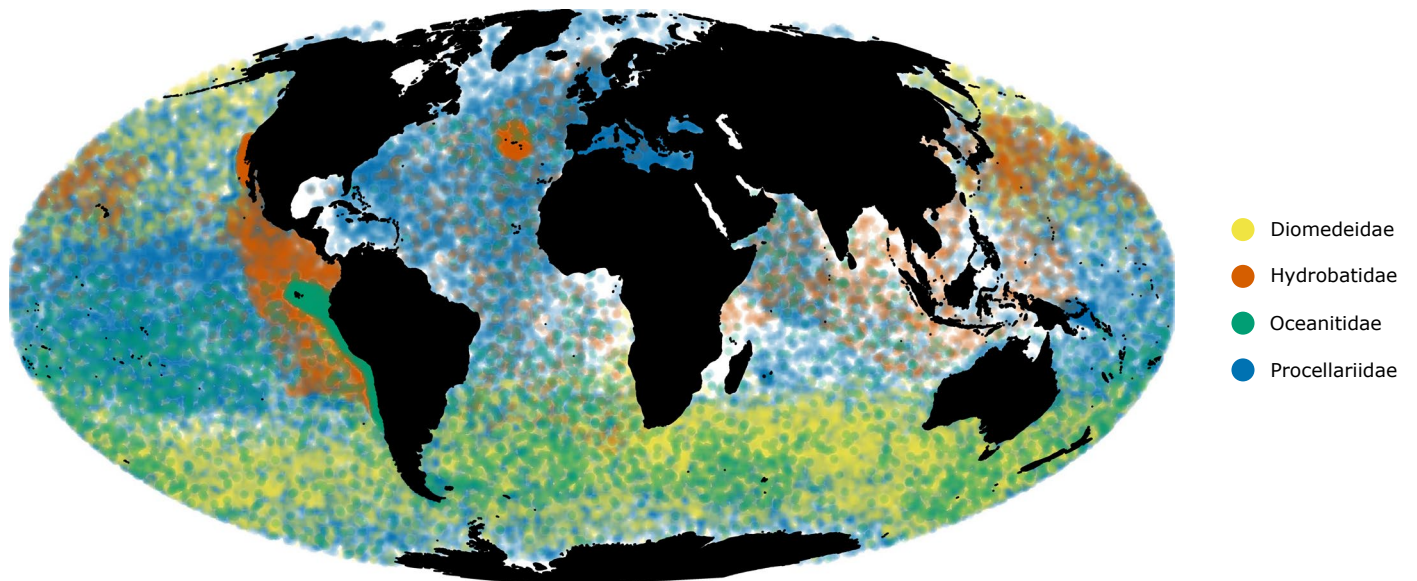
Extended Data Fig. 1 | Bivariate phylogenetic regression of seabird body mass against sea surface temperature. Sea surface temperature has a significant negative effect on body mass ($pMCMC_{100} > 95$) but explains only 6% of the

variance, suggesting additional factors influence mass diversity in seabirds. The solid black line shows the mean regression slope estimated from the posterior distribution ($n = 120$ species).

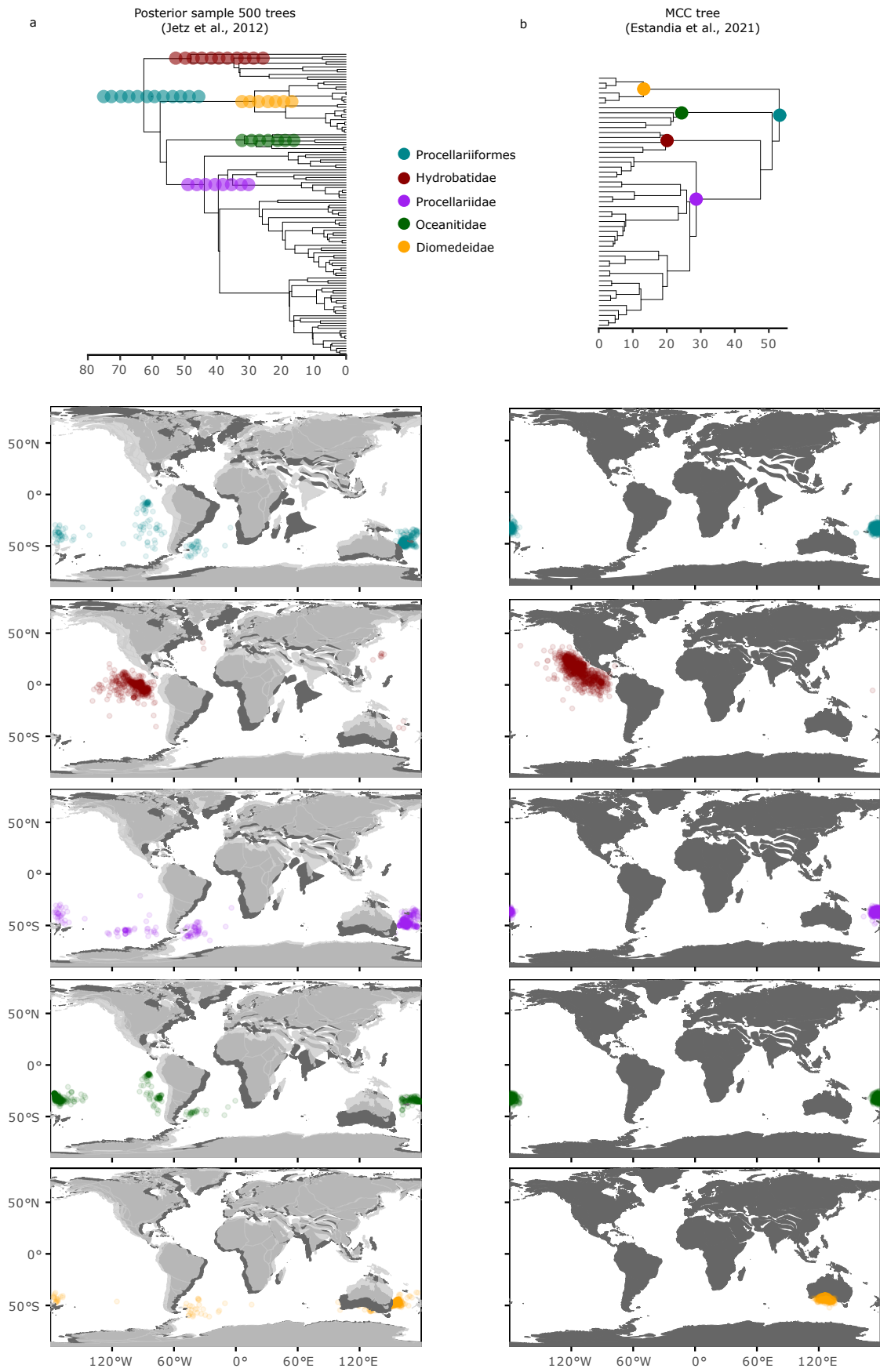


Extended Data Fig. 2 | DensiTree from Jetz phylogeny. Dated trees are superimposed with consistent tip ordering. Vertical dashed lines mark the ages of the climatic layers used to extract two-meters palaeotemperature

at reconstructed phylogenetic node-locations. Downstream analyses were performed across this sample of trees to assess robustness to phylogenetic uncertainty ($n = 120$ species; 500 trees).



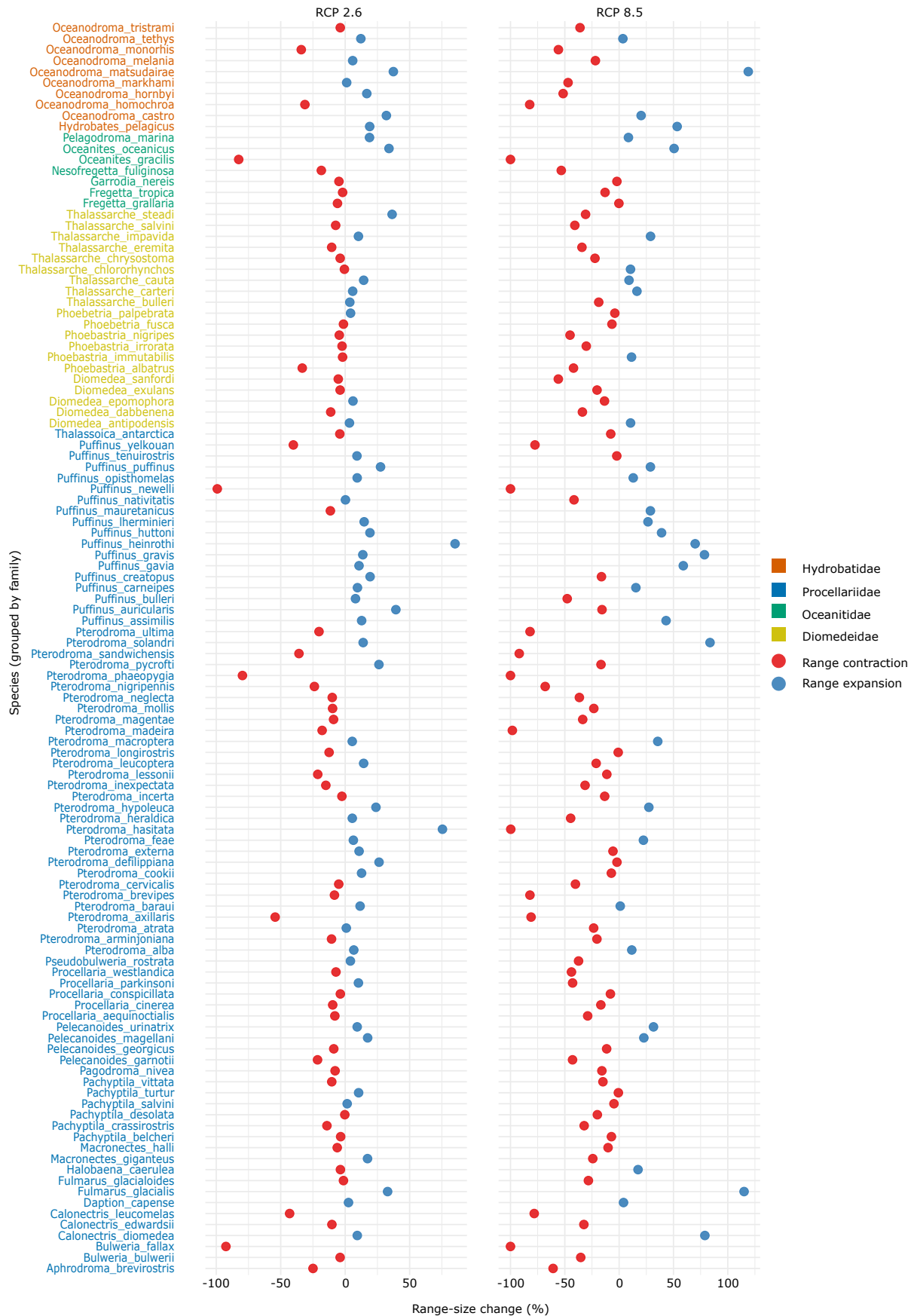
Extended Data Fig. 3 | Global geographic distribution records for Procellariiformes. Semi-transparent dots show the randomly generated coordinates within BirdLife range polygons. These points were used in downstream analyses (n = 58,350 coordinates, 120 species).



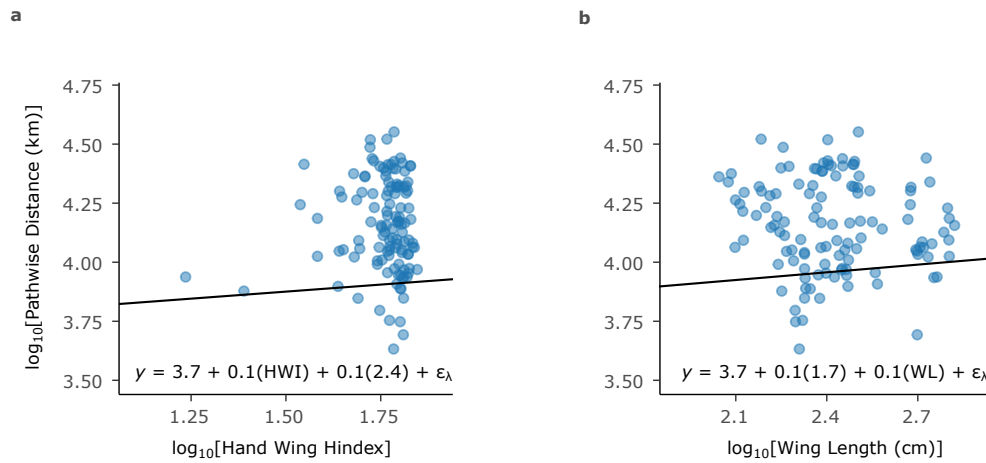
Extended Data Fig. 4 | See next page for caption.

Extended Data Fig. 4 | Ancestral geographic locations for deeper nodes in Procellariiformes inferred using the Geo model. a. Results based on 500 phylogenetic trees from Jetz et al. (2012). The maximum clade credibility (MCC) tree is shown for reference. Transparent points on the MCC tree indicate the range of node ages for the root and four families across the posterior sample. Dark and light palaeomaps correspond to the oldest and youngest node ages,

respectively. Transparent points on the maps show median node coordinates from the posterior distribution (n = 500 median coordinates per node). **b.** Results based on the MCC tree from Estandia et al. (2021). Dark palaeomaps correspond to node ages on the MCC tree. Transparent points show the posterior distribution of node coordinates (n = 500 coordinates per node).



Extended Data Fig. 5 | Projected changes in range size by 2100 under two climate-change scenarios. The plot shows the best-fitting (out of five) species distribution model for each species (selected by AUC). Projections are presented for the low-emissions (RCP 2.6) and high-emissions (RCP 8.5) scenarios (n = 114 species).



Extended Data Fig. 6 | Pathwise distance is independent of two metrics of dispersal ability in seabirds. Neither **a**, hand-wing index ($pMCMC_{73} < 95$) nor **b**, wing length ($pMCMC_{75} < 95$) is significantly associated with pathwise distance. Solid black lines show mean regression slopes estimated from the posterior distribution ($n = 120$ species).

Extended Data Table 1 | Evolutionary model fitting for phylogenetic regressions

Regression model	Lh. BM	Lh. LA	Lh. VR	Lh. VRLA	Lh. OU
Body mass $\sim \alpha + \beta_1(\text{Range size})$	8.8	4.5	9.8	4.8	4.0
Range size $\sim \alpha + \beta_1(\text{LT}_{\text{RATE}}) + \beta_2(\text{LT}) + \beta_3(\text{Body mass})$	-148.1	-133.1	-121.8	-124.1	-131.31
Pathwise distance $\sim \alpha + \beta_1(\text{LT}_{\text{RATE}}) + \beta_2(\text{Range Size}) + \beta_3(\text{LT}_{\text{RATE}} * \text{Range size})$	32.3	36.7	37.8	36.3	NA
Speciation rate $\sim \alpha + \beta_1(\text{LT}_{\text{RATE}}) + \beta_2(\text{Body mass})$	172.3	165.3	NA	NA	NA

The log Marginal Likelihood (Lh), estimated by stepping stone sampling, provides the models support given the data and priors. The best fitting model is highlighted in bold. BM = Brownian Motion, LA = Lambda, VR = Variable Rate, VRLA = Variable Rate and Lambda, OU = Ornstein-Uhlenbeck, LT = local temperature, LT_{RATE} = rate of local temperature change, Pathwise distance = extant species geographic distances travelled from the location of the common ancestor. Speciation rate = node count along the species phylogenetic paths. (n=120 body mass, range size, LT, and speciation rate; 60,000 LT_{RATE} and Pathwise distance).

Extended Data Table 2 | Phylogenetic regression analyses using the phylogeny of Estandia et al (2021)

Response	Predictors
Range size	$\alpha - \beta_1(LT_{RATE}) - \beta_2(LT) + \beta_3(\text{Body Mass})$
Pathwise distance	$\alpha + \beta_1(LT_{RATE}) - \beta_2(\text{Range Size}) - \beta_3(LT_{RATE} * \text{Range Size})$
Speciation rate	$\alpha + \beta_1(LT_{RATE}) + \beta_2(\text{Body Mass})$

Significant beta coefficients (pMCMC > 95%) are in bold. LT_{RATE} = rate of local temperature change, LT = local temperature, Pathwise distance = extant species geographic distances travelled from the location of the common ancestor. (n=51 Range size, Body Mass, LT, and Speciation rate data. n=25,500 LT_{RATE} and Pathwise distance data).

Reporting Summary

Nature Portfolio wishes to improve the reproducibility of the work that we publish. This form provides structure for consistency and transparency in reporting. For further information on Nature Portfolio policies, see our [Editorial Policies](#) and the [Editorial Policy Checklist](#).

Statistics

For all statistical analyses, confirm that the following items are present in the figure legend, table legend, main text, or Methods section.

n/a Confirmed

- The exact sample size (n) for each experimental group/condition, given as a discrete number and unit of measurement
- A statement on whether measurements were taken from distinct samples or whether the same sample was measured repeatedly
- The statistical test(s) used AND whether they are one- or two-sided
Only common tests should be described solely by name; describe more complex techniques in the Methods section.
- A description of all covariates tested
- A description of any assumptions or corrections, such as tests of normality and adjustment for multiple comparisons
- A full description of the statistical parameters including central tendency (e.g. means) or other basic estimates (e.g. regression coefficient) AND variation (e.g. standard deviation) or associated estimates of uncertainty (e.g. confidence intervals)
- For null hypothesis testing, the test statistic (e.g. F , t , r) with confidence intervals, effect sizes, degrees of freedom and P value noted
Give P values as exact values whenever suitable.
- For Bayesian analysis, information on the choice of priors and Markov chain Monte Carlo settings
- For hierarchical and complex designs, identification of the appropriate level for tests and full reporting of outcomes
- Estimates of effect sizes (e.g. Cohen's d , Pearson's r), indicating how they were calculated

Our web collection on [statistics for biologists](#) contains articles on many of the points above.

Software and code

Policy information about [availability of computer code](#)

Data collection

Data analysis https://www.evolution.reading.ac.uk/BayesTraitsV5.0.3/BayesTraitsV5.0.3.html (version 5)
<https://github.com/AndrewPMeade/BayesTraits-Release> (version 5)
<https://www.r-project.org/> (version 4.5.3)"/>

For manuscripts utilizing custom algorithms or software that are central to the research but not yet described in published literature, software must be made available to editors and reviewers. We strongly encourage code deposition in a community repository (e.g. GitHub). See the Nature Portfolio [guidelines for submitting code & software](#) for further information.

Data

Policy information about [availability of data](#)

All manuscripts must include a [data availability statement](#). This statement should provide the following information, where applicable:

- Accession codes, unique identifiers, or web links for publicly available datasets
- A description of any restrictions on data availability
- For clinical datasets or third party data, please ensure that the statement adheres to our [policy](#)

The authors declare that data supporting the finding are available at figshare <https://doi.org/10.6084/m9.figshare.29900165>

Research involving human participants, their data, or biological material

Policy information about studies with [human participants or human data](#). See also policy information about [sex, gender \(identity/presentation\), and sexual orientation](#) and [race, ethnicity and racism](#).

Reporting on sex and gender

Reporting on race, ethnicity, or other socially relevant groupings

Population characteristics

Recruitment

Ethics oversight

Note that full information on the approval of the study protocol must also be provided in the manuscript.

Field-specific reporting

Please select the one below that is the best fit for your research. If you are not sure, read the appropriate sections before making your selection.

Life sciences Behavioural & social sciences Ecological, evolutionary & environmental sciences

For a reference copy of the document with all sections, see [nature.com/documents/nr-reporting-summary-flat.pdf](https://www.nature.com/documents/nr-reporting-summary-flat.pdf)

Ecological, evolutionary & environmental sciences study design

All studies must disclose on these points even when the disclosure is negative.

Study description

Research sample

Sampling strategy

Data collection

Timing and spatial scale

Data exclusions

Reproducibility

Randomization

Blinding

Did the study involve field work? Yes No

Reporting for specific materials, systems and methods

We require information from authors about some types of materials, experimental systems and methods used in many studies. Here, indicate whether each material, system or method listed is relevant to your study. If you are not sure if a list item applies to your research, read the appropriate section before selecting a response.

Materials & experimental systems

- n/a | Involved in the study
- Antibodies
 - Eukaryotic cell lines
 - Palaeontology and archaeology
 - Animals and other organisms
 - Clinical data
 - Dual use research of concern
 - Plants

Methods

- n/a | Involved in the study
- ChIP-seq
 - Flow cytometry
 - MRI-based neuroimaging

Plants

Seed stocks	<input type="text" value="n/a"/>
Novel plant genotypes	<input type="text" value="n/a"/>
Authentication	<input type="text" value="n/a"/>